

Multi-messenger Approach to Ultra-light Scalars

Indra Kumar Banerjee, Soumya Bonthu, Ujjal Kumar Dey

Department of Physical Sciences, Indian Institute of Science Education and Research
Berhampur,

Transit Campus, Government ITI, Berhampur 760010, Odisha, India

E-mail: indrab@iiserbpr.ac.in, bonthu19@iiserbpr.ac.in, ujjal@iiserbpr.ac.in

Abstract. We propose a novel method to study the ultra-light scalars, where compact rotating objects undergo the phenomenon of superradiance to create gravitational waves and neutrino flux signals. The neutrino flux results from the ‘right’ coupling between the ultra-light scalars and the neutrinos. We study the intertwining of gravitational waves and neutrino flux signals produced from a single source and elaborate if and when the signals can be detected in existing and upcoming experiments in a direct manner. We also discuss an indirect way to test it by means of cosmic neutrino background which can be detected by upcoming PTOLEMY experiment.

Contents

1	Introduction	1
2	Consequences of Black Hole Superradiance	3
2.1	Generation of Gravitational Waves	4
2.2	Generation of Neutrino Flux	5
3	Results	6
3.1	Combination of the Two Messengers	6
3.2	Direct Signals	7
3.3	Indirect Effect: Complimentary Search	8
4	Summary and Conclusion	10

1 Introduction

The current parlance of fundamental physics suffers from the lack of information regarding two of its most important components, i.e. neutrinos and dark matter. The unanswered questions regarding neutrinos are the origin and absolute value of its mass as well as its nature i.e., whether they are Dirac or Majorana type particles. Many experimental efforts are underway to probe neutrinos from various sources across a large range of energy varying all the way from sub-meV to a few thousands of PeV [1–30]. Interestingly, neutrinos can be an excellent messenger due to its abundance, originated from astrophysical, terrestrial, cosmological and other sources [31–40], and its weakly interacting nature which allows almost unhindered propagation of cosmological length scales. Consequently neutrinos can retain most of the information regarding their sources and the environment it travels through. Thus a lot of progress has been made to probe neutrinos from extra-terrestrial sources and many other experiments are being planned and invested on to widen the range of neutrinos that we can observe.

For dark matter, the scope is even wider as there is a myriad of theories where dark matter can be of particulate nature, or some exotic compact object and even a combination of both. For the particulate dark matter, the mass can vary from $\mathcal{O}(10^{-24})$ eV to a few hundreds TeV [41, 42]. For extremely tiny masses, i.e., the ultra-light domain (10^{-24} eV – 1 eV) it is extremely difficult to probe them directly in laboratory experiments and therefore we have to rely on indirect means. The bosons¹ in this mass range specifically intrigues the community as the QCD axions and various axion-like particles (ALP) reside in this domain. For example, in string theoretic scenarios compactification can give rise to many different ALPs and they form an ‘axiverse’, some of which also stay in this mass domain [43]. There can be scalars even lighter than 10^{-24} eV and while they can not play the role of dark matter, they are still viable candidates for dark energy [44]. Furthermore, ultra-light scalars can also be the mediator of a long range ‘fifth force’ [45]. Due to this versatility of the ultra-light scalars (ULS), it is very interesting to probe them to gain information about their properties, more precisely their interaction with the standard model (SM) sector. While direct

¹In this article we just focus on the scalars. Moreover the underlying processes involved are independent of whether it is scalar or pseudoscalar, so we will not distinguish between them anywhere in the text.

detection of ULS is unfeasible, the indirect effects originating from astrophysical or cosmic events, such as cosmic birefringence [46–48], axion(ALP)-photon conversion around a compact object [49], gravitational waves [50], and neutrino flux [51] generated from superradiance around a compact object, etc. can come to the rescue. In this study, we focus on the last one, i.e., gravitational waves (GW) and neutrino flux originating from superradiance around a compact object. However, the generation of neutrino flux depend upon the coupling, if any, between the neutrinos and the ULS [51]. It is worth mentioning here that a coupling of this type between ultra-light bosonic field and neutrinos proposed due to various motivations such as generation of neutrino mass [52], grand unified theory [53–55] etc.

Superradiance is a theoretical prediction which can spontaneously create bosons around a rotating compact object [56, 57]. In this study, we consider rotating black holes (BH) to be the origin of such superradiance and we consider BSM ultra-light scalar degrees of freedom. These scalars can form a cloud around the rotating BH under certain conditions forming a bound system with discrete energy levels [58]. GW can be produced from this in two-fold ways, namely, due to the transition of ULS from one energy level to another, and their annihilation to the gravitons [50]. In this regard, it is worth mentioning that, GW, which was just a theoretical prediction less than a decade ago, has been observed first by the LIGO collaboration in 2016 and since then almost a hundred GW events have been observed, which were transient in nature and astrophysical in origin [59]. Recently the pulsar timing arrays (PTA) have shown hints of GWs which are stochastic in nature [60–68], i.e. they are GW background which might be of astrophysical or cosmological in nature. A number of upcoming interferometer based GW detectors e.g., LISA [69], Taiji [70], DECIGO [71], BBO [72], ET [73], CE [74], and in the ultra-high frequency domain detectors based on the principle of mechanical resonators (LSD) [75, 76], GW-electromagnetic wave conversion [77–80], resonant L-C circuits(DMR) [81, 82], interferometry [83, 84], gaussian beam (GB) [85–87], radio telescope [88, 89] etc. will only flourish this burgeoning field of GW astronomy. Moreover, multi-messenger astronomy with already existing astronomical messengers like photons, cosmic rays, neutrinos, will greatly be augmented by the arrival of GW astronomy.

In this article, we aim to probe the ultra-light scalars and more importantly its coupling with the active neutrinos (if any) through multi-messenger astronomy. The main scheme is as follows. We consider the source of ULS as the spinning BH which can undergo superradiant instability that leads to the formation of a cloud of ULS around them [56, 57]. This formation however depends on the product of the masses of the ULS and the BH. We briefly discuss the mechanism in Sec. 2. Next we consider the constituent messengers, i.e. (a) the transient GW originating from the annihilation of the scalars into gravitons [50] and (b) the neutrino flux which may be generated from the scalar cloud provided that there is appropriate Yukawa coupling between the neutrinos and the ULS [51]. We then discuss the dependence of these two ‘direct signals’, i.e. signals which are generated from the scalar cloud, on the various parameters of the source BH e.g. luminosity distance (d), mass (M_{BH}), spin (χ), and the properties of the scalar e.g. mass (m_ϕ), coupling with the neutrinos ($g_{\nu\phi}$). One of the novel features of the study is that two messengers arising from the same source are considered in combination to determine the properties of ULS which would otherwise be impossible to probe. Furthermore, it is to be noted here that though these two messengers from BH superradiance have separately been studied, our study is the first one to give a prescription on how to effectively use both of them in consonance to shed some light on the ULS. Previously mentioned coupling between the scalar and the neutrinos will also have other phenomenological implications. For the relevant parameter space we consider the modification of the cosmic

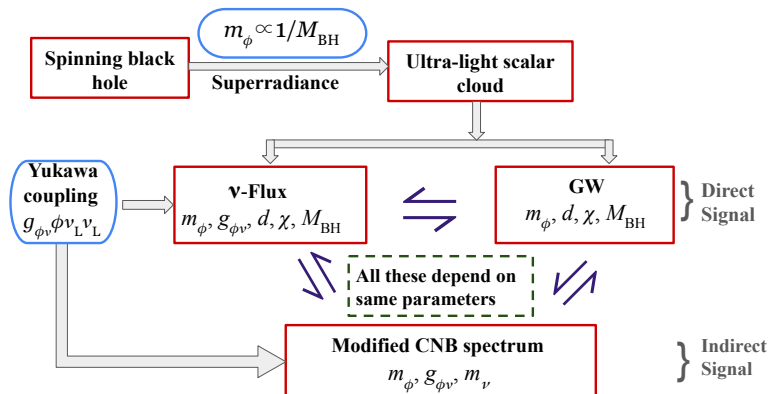


Figure 1: Diagram displaying the main scheme of this article. The blue boxes signify the inputs from the ULS properties. The direct and the indirect signals have been specified. The variable on which each signal depends have also been shown.

neutrino background (CNB) spectra due to decay of the heavier neutrino mass eigenstate to lighter ones through the channel of this Yukawa coupling. We term this as an ‘indirect signal’ as this does not originate from the source BH but can still aid in probing the scalar properties. In Fig. 1 we schematically show the underlying motif of the work.

This article is organized as follows. In Sec. 2 we explain in details the mechanism of the origin of the creation of GW and neutrino flux from the superradiance respectively. In Sec. 3 we explain our finding with the help of a few benchmark cases. Finally in Sec. 4 we summarize and conclude.

2 Consequences of Black Hole Superradiance

Superradiance is a phenomenon, through which ultra-light bosons can form a cloud around a rotating compact object if the angular momentum of the rotating compact object is high enough to trigger it [56, 57]. Essentially the scalar field amplifies around the compact object through the extraction of energy and angular momentum. In this study, we focus on ULS cloud forming around rotating black holes. The scalar cloud can be gravitationally bound to the rotating BH to form a bound system with discrete energy levels. This system is analogous to a hydrogen atom and hence it is termed as ‘gravitational atom’. The efficiency of the superradiance process, i.e. the creation of the ultra-light scalar cloud, depends on the ratio of the gravitational radius of the BH and the Compton wavelength of the scalar which is called as gravitational fine structure constant α_g and can be expressed as a combination of the mass of the scalar and the BH [90],

$$\alpha_g = \frac{GM_{\text{BH}}m_\phi}{\hbar c}, \quad (2.1)$$

where G is the Newton’s gravitational constant, m_ϕ is the mass of the scalar and M_{BH} is the mass of the BH. The superradiance is negligible if the α_g is too small whereas it is the most efficient when $\alpha_g \sim \mathcal{O}(1)$ [90]. However, we take the conservative approach and throughout this article, we consider α_g to be $\mathcal{O}(0.1)$. From that aspect, we can find the mass range for the black holes in question which will superradiate ultra-light scalars (within the mass range

between 10^{-24} eV and 1 eV) to be between $10^{14}M_\odot$ and $10^{-10}M_\odot$. Therefore, very small portion of this range can be astrophysical in nature while most of the range is within the primordial or supermassive domain. However, we remain agnostic regarding the nature of the BH in this study. Once these conditions are met, superradiance occurs due to the transfer of angular phase velocity from the BH to the states of a massive scalar, which amplifies the field value of the scalar in question. The ground state of the ULS takes the form [90],

$$\Phi(\vec{x}, t) = \Psi_0(t)R_{\alpha_g}(r) \sin\theta \cos(m_\phi t - \phi), \quad (2.2)$$

where Ψ_0 is the peak field value and $R_{\alpha_g}(r)$ is the normalized radial solution. After the superradiance is triggered the ULS will eventually form the cloud whose mass is related to the peak field value as [51],

$$M_S = \frac{186\Psi_0^2}{\alpha_g^3 m_\phi}. \quad (2.3)$$

It is worth mentioning here that we consider $M_S \sim 0.1M_{\text{BH}}$ because if the cloud is heavier than this then the spin of BH will go lower than the threshold required for superradiance and it will come to a halt [51].

Now we move to the consequences of the black hole superradiance. In this article, we mainly focus on the generation of GW and neutrino flux and we briefly discuss the methods as follows.

2.1 Generation of Gravitational Waves

There are multiple ways in which GW can be generated from BH superradiance, e.g., annihilation of the scalars to gravitons, transition of the energy levels of the gravitational atom [50], from bosonova [91], etc. For simplicity here we only consider the annihilation of the scalars into gravitons. Furthermore, these GW can be either of transient nature, i.e. lasts for a finite time or they can be a stochastic background. Therefore it requires a comprehensive analysis regarding the BH population throughout all sky to take the entire population of BH into account to incorporate all the possible sources into the analysis to predict the resultant GW spectra, which we leave for future work. In the present case we consider transient monochromatic GW and the rate of energy released in the form of GW can be expressed as [92],

$$\dot{E}_{\text{GW}} \propto \left(\frac{M_S}{M_{\text{BH}}}\right)^2 \alpha_g^{4l+4s+10}, \quad (2.4)$$

where l and s are the angular and spin quantum number. It is worth mentioning here that since in our work we consider $\alpha < 1$, the rate of energy extracted by the scalar cloud is much larger than the energy radiated in the form of GW [92]. The frequency of the GW released can be expressed as [90],

$$f_{\text{GW}} \sim 5 \left(\frac{m_\phi}{10^{-12} \text{ eV}}\right) \text{ kHz}. \quad (2.5)$$

Since this is transient GW, the duration of the dominant mode in case of the scalar cloud is [92],

$$\tau_{\text{GW}} = 1.3 \times 10^5 \left(\frac{M_{\text{BH}}}{M_\odot}\right) \left(\frac{0.1}{\alpha_g}\right)^{15} \left(\frac{0.5}{\chi_i - \chi_f}\right) \text{ yr}, \quad (2.6)$$

where χ_i and χ_f are the initial and final BH spin. As mentioned before, if only the dominant hydrogenic mode is considered, then the GW strain can be approximated as [92],

$$h_{\text{GW}} = 5 \times 10^{-27} \left(\frac{M_{\text{BH}}}{10M_{\odot}} \right) \left(\frac{\alpha_g}{0.1} \right)^7 \left(\frac{\text{Mpc}}{d} \right) \left(\frac{\chi_i - \chi_f}{0.5} \right), \quad (2.7)$$

where d is the luminosity distance. Also, in the detector frame the frequency of the gravitational waves are redshifted as $f = f_{\text{GW}}/(1+z)$ where z is the cosmological redshift of the source. However, in our case, all the benchmark sources we consider, have $z \leq 0.01$, and therefore the frequency in the source and the detector frame can be approximately taken equal to each other².

2.2 Generation of Neutrino Flux

As mentioned before, ultra-light scalars can be produced due to superradiance of BH and can form a cloud around the BH. In this section we discuss the origin of neutrino flux from this scalar cloud if there exists a coupling between the neutrinos and the scalars of the form $g_{\phi\nu}\phi\nu_L\nu_L$ where ν_L denotes the active neutrinos [93]. Several cosmological observations, e.g., supernova cooling, CMB etc. put bound on this coupling, $g_{\phi\nu} < 3 \times 10^{-7}$ [94–98]. For simplicity we assume this coupling to be democratic to all neutrino eigenstates.

Due to this coupling and the high field values of the scalar, the neutrinos realize an extra mass term $g_{\phi\nu}\phi$ which is of oscillating nature due to the time varying nature of the ϕ field shown in Eq. (2.2). When the effective mass of the neutrino crosses zero, the neutrinos are produced through parametric excitation. These neutrinos then follow the geodesic which is effected by the Kerr metric and the oscillating mass term. Subsequently the neutrinos are accelerated to much higher energy than the one it was produced and hence the Pauli blocking does not come into play to interfere with the production of the subsequent neutrinos. See Ref. [51] and references therein for further details of this process.

The average energy and the differential flux for a distant observer of the neutrinos generated from the above-mentioned process can be expressed as [51],

$$E_{\nu} \approx 2.7 \left(\frac{g_{\phi\nu}}{10^{-8}} \right) \left(\frac{\Psi_0}{10^{12} \text{ GeV}} \right) \text{ TeV}. \quad (2.8)$$

$$\begin{aligned} \Phi_{\nu} \approx & 1.2 \times 10^{-17} \left(\frac{g_{\phi\nu}}{10^{-8}} \right)^{1/2} \left(\frac{\Psi_0}{4.8 \times 10^7 \text{ GeV}} \right)^{1/2} \\ & \times \left(\frac{10^{-12} \text{ eV}}{m_{\phi}} \right)^{1/2} \left(\frac{0.3}{\alpha_g} \right)^3 \left(\frac{10 \text{ kpc}}{d} \right)^2 \text{ cm}^{-2}\text{s}^{-1}\text{eV}^{-1}. \end{aligned} \quad (2.9)$$

It can be seen that both of these quantities depend directly on the peak field value. Moreover, the critical peak field value (Ψ_0^c) of the scalar can be found using the condition that the energy provided to the scalar cloud by the BH is taken away by the neutrino and it can be expressed as [51],

$$\Psi_0^c = 4.8 \times 10^7 \left(\frac{m_{\phi}}{10^{-12} \text{ eV}} \right) \left(\frac{\alpha_g}{0.3} \right)^{16} \left(\frac{10^{-7}}{g_{\phi\nu}} \right)^5 \left(\frac{\chi_i}{0.9} \right)^2 \text{ GeV}. \quad (2.10)$$

²The luminosity distance can be expressed as a function of redshift as $d \approx (c/H_0)z$. In the later part of this article, we have considered a few benchmark cases, among which the furthest source we have considered is at a distance of 50 Mpc.

Since we are equipped with the expressions which quantify the dependence of these signals on the source parameters, now we move on to explicitly understand the interplay between these two messengers in the next section.

3 Results

As mentioned in the previous section, the same source can create two different messengers and the properties of both of these messengers depend on the same parameters. We first discuss a possible interplay of the GW signal and neutrino flux to get deeper insight on the source. In order to emphasise on this, we consider a few benchmark cases to specifically show the imprints of certain source configurations on the upcoming and current GW and neutrino detectors. Finally, as a mode of a complimentary search, we show the effect of the coupling between the neutrinos and the ultra-light scalar, which is responsible for the creation of the neutrino flux from the BH, on the detector of cosmic neutrino background (CNB).

3.1 Combination of the Two Messengers

The dependence of the neutrino flux and energy along with GW strain and frequency on the source parameters, such as mass of the BH, the gravitational fine structure constant, luminosity distance of the source, and the spin of the BH is of pivotal importance as they can pave a way to connect the two messengers, GW and neutrino signals, which would otherwise seem to be independent of each other.

The left panel of Fig. 2 is a bandplot of gravitational wave frequency and neutrino energy for different values of coupling. For this we have considered the $\alpha_g = 0.25$ and $\chi_i = 0.9$. From this plot we find that the gravitational wave frequency and neutrino energy have a linear dependence in the log scale. The energy-axis intercept of the graph corresponds to the coupling between the neutrinos and ULS ($g_{\nu\phi}$). It is also observable that the energy of neutrino and the coupling has an inverse relation, i.e. high energy neutrinos signify low coupling at constant gravitational wave frequency. This partially signifies how the two messengers can be put to work to understand the highly sought after coupling between the neutrinos and the ultra-light scalar.

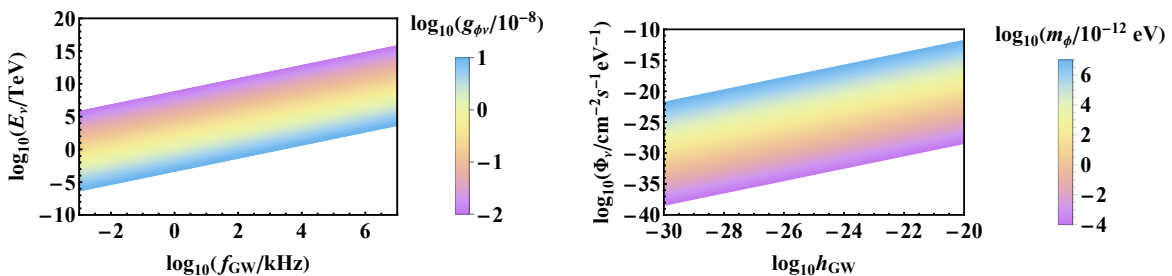


Figure 2: (Left) The relation of gravitational wave frequency and neutrino flux energy with varying coupling $g_{\nu\phi}$. (Right) The relation of gravitational wave strain and neutrino flux with varying mass of the ultra-light scalar.

In the right panel of Fig. 2, it is prominent that, gravitational wave strain is directly proportional, in the logarithmic scale, to the neutrino flux generated and the intercept signifies the mass of the ULS. Neutrino flux and mass of the ultralight scalar has a direct dependence, i.e. higher flux corresponds to higher mass for constant gravitational wave strain.

3.2 Direct Signals

To further illustrate the versatility and the range of this method, we show a few specific scenarios for which both the signals will be relevant. We consider four benchmark cases and discuss their imprint in the neutrino flux-energy and gravitational wave frequency-strain space. The benchmark cases are shown in Tab. 1. The source of the first BP is motivated from BHs of astrophysical nature, the second BP is motivated by primordial black holes whereas the third and fourth BPs are motivated by supermassive BHs. The distance of the BHs from the earth has been taken with a conservative approach, i.e., the shortest distance considered in the benchmark cases is much larger than the distance of the BH closest to earth which is at a distance of 480 pc [99]. It is to be noted that the benchmark parameters are considered in such a way that the resulting GW and neutrino flux can be at a level which is in the reach of upcoming GW and neutrino detectors respectively.

BP	$M_{\text{BH}} (M_{\odot})$	α_g	$g_{\phi\nu}(\times 10^{-8})$	$\chi_i - \chi_f$	d (Mpc)
1	10^2	0.2	0.3	0.5	0.1
2	3×10^{-6}	0.23	3	0.5	0.1
3	10^4	0.25	0.02	0.5	10
4	10^6	0.25	0.2	0.5	50

Table 1: Benchmark parameters for the BH sources and the coupling constants which can lead to direct signals.

The signals arising from the BPs given in Tab. 1, are shown in Figs. 3 and 4 in the GW frequency-strain and neutrino flux-energy space, respectively. We describe the properties of the signals from each of these BPs as follows. For the case of BP 1, the gravitational wave frequency, $f_{\text{GW}} \sim 10^3$ Hz and the gravitational wave strain, $h_{\text{GW}} \sim 10^{-22}$, which is in the sensitivity range of the ET. The neutrino flux produced for the same will be, $\Phi_{\nu} \sim 10^{-18} \text{ cm}^{-2}\text{s}^{-1}\text{eV}^{-1}$ with the energy, $E_{\nu} \sim 10^{14}$ eV. This energy is in the ballpark of high-energy atmospheric neutrinos, however, the flux value is much larger than the flux of the atmospheric neutrinos which suggests that a presence of such a signal will be not be cloaked by the atmospheric neutrinos. BP 2 corresponds to the gravitational wave frequency, $f_{\text{GW}} \sim 10^{10}$ Hz and the gravitational wave strain, $h_{\text{GW}} \sim 10^{-30}$ which is in the reach of gaussian beam (GB) experiments. The corresponding neutrino flux, $\Phi_{\nu} \sim 10^{-12} \text{ cm}^{-2}\text{s}^{-1}\text{eV}^{-1}$ with the neutrino energy, $E_{\nu} \sim 10^{19}$ eV. This is in the range of cosmogenic neutrinos but the flux is many orders of magnitude higher. For BP3, we obtain the resultant GW with $f_{\text{GW}} \sim 10^2$ Hz and $h_{\text{GW}} \sim 10^{-21}$, whose signature can be probed in ET. The neutrino flux from the same will be, $\Phi_{\nu} \sim 10^{-21} \text{ cm}^{-2}\text{s}^{-1}\text{eV}^{-1}$ with energy $E_{\nu} \sim 10^{18}$ eV. These neutrinos, like the previous case, are also in the range of the cosmogenic neutrino and has much higher flux than them and therefore will be detectable. Finally for BP4, the GW has $f_{\text{GW}} \sim 0.1$ Hz and $h_{\text{GW}} \sim 10^{-20}$, hence it will be in the range of LISA detector. However, the neutrino flux will be $\Phi_{\nu} \sim 10^{-22} \text{ cm}^{-2}\text{s}^{-1}\text{eV}^{-1}$ and their energy will be $E_{\nu} \sim 10^{12}$ eV and thus these neutrinos will remain enshrouded by the atmospheric neutrinos in the same energy range.

It is worth mentioning that benchmark parameters considered in our study lie in the energy range of 10^{12} eV to 10^{19} eV. Some other sources of neutrinos with the same energy range include, active galactic nuclei (AGN) [100], the galactic plane [101], gamma ray bursts [102], radio-emitting tidal disruption events, [103] and accretion flares from massive black holes [104], etc. But the flux associated with the same resides in the cosmogenic neu-

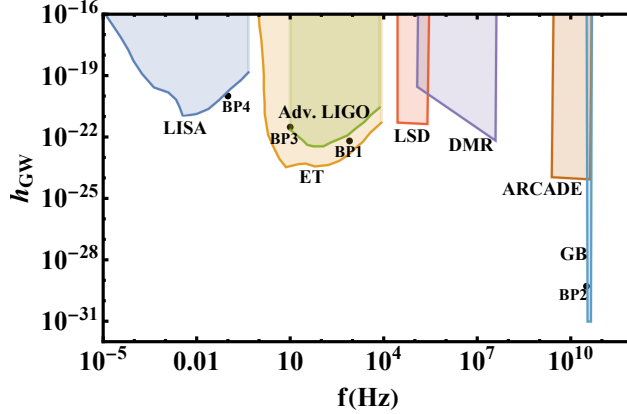


Figure 3: The GW created due to the four benchmark cases in Tab. 1. We also show the sensitivity curves of the current and future GW experiments in the relevant frequency range.

trino flux range as opposed to the flux generated for our benchmark cases in general. The detection of these ultra-high energy neutrinos are being carried out by currently-working and proposed experimental setups like IceCube [12], RNO-G [14] and GRAND [30].

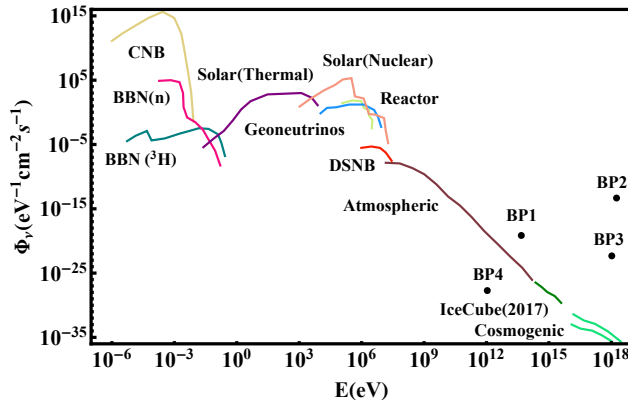


Figure 4: The neutrino flux created due to the four benchmark cases in Tab. 1. We also show the other sources of neutrinos in the flux-energy space.

These benchmark cases illustrate the efficiency of considering both the signals from the same source as an avenue to extract pinpointed information from them. However, it is not devoid of ambiguity, i.e. due to the involvement of many parameters, there could be multiple combination of source BH properties and coupling which can lead to signals in the same ballpark. In order to remove some of that ambiguity, we look into a complimentary mode of investigation which only gets affected by the coupling.

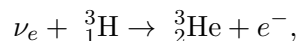
3.3 Indirect Effect: Complimentary Search

For the purpose of complimentary search, we use CNB neutrinos to probe the effect of the coupling $g_{\phi\nu}$ which is crucial for our study. According to the standard cosmology and the standard model of particle physics, neutrinos decoupled around one second after the big bang and are freely streaming through the universe without interacting with almost anything

since then. In this section, we show the modification in the distribution of the different mass eigenstates of CNB neutrinos taking the effect of the ULS into account.

As neutrinos are now proven to be massive particles, under specific conditions they may have finite lifetime. We take into consideration the Majorana nature of the neutrinos and assume the decay to be visible, i.e., though the other daughter particles are undetectable, the lighter neutrino is detectable. Here we assume the simple case of 2-body decay where the heavy i -th mass eigenstate of neutrinos decay to lighter j -th mass eigenstate [105–107]. This process can be expressed as, $\nu_i \rightarrow \nu_j + \phi$ where ϕ is the ULS we are interested in this study. In the presence of this decay the dynamics of CNB is governed by not only the neutrino mass but also the scalar mass and the coupling $g_{\phi\nu}$. In the underlying interaction $g_{\phi\nu}\phi\nu_L\nu_L$ or $g_{\phi\nu}^{ij}\phi\nu_i\nu_j$, the $g_{\phi\nu}^{ij}$ contains the information regarding interaction strength and the PMNS matrix elements. Recall that the same interaction, i.e., $g_{\phi\nu}\phi\nu_L\nu_L$ also caused the creation of the neutrinos from the BH superradiance as explained in Sec. 2.2. Throughout our study, we have assumed the coupling between neutrinos and ultra-light scalars $g_{\phi\nu} \in [0.01, 1] \times 10^{-8}$. As a result of this in normal hierarchy ν_3 will decay into ν_1 and ν_2 in relatively shorter time period than the age of the universe. In case of inverted ordering, ν_2 decays into ν_1 and ν_3 . For simplicity we just show this effect for the case of normal ordering though the same can be extended to inverted ordering as well.

Till date the best bet in detecting the CNB neutrinos is the proposed detector PTOLEMY which is based on the mechanism of neutrino capture on tritium atom [108]. The basic process that governs this detector is,



neutrinos are captured by the tritium atom to produce helium atom and an electron. The differential energy spectrum of these electrons can lead us to the energy distribution and thus the decay possibilities of the incoming CNB neutrinos. It is worth mentioning that in principle there is no lower bound of the threshold energy of the neutrinos for the capture process to occur. There are however a few difficulties in the actual execution of the idea experimentally. This is mainly due to the Heisenberg’s uncertainty principle which makes it extremely difficult to lower the resolution of the experiment. In such a scenario it is very challenging distinguish the electron spectra arising from the neutrino capture and the background electrons spectra created due to the β -decay of the tritium [109]. However, these difficulties are being tried to overcome [110].

We show the electron spectra predicted for PTOLEMY in Fig. 5 where we have assumed an experimental resolution of 40 meV, the ν_3 mass of 50 meV, m_ϕ as 0.001 meV and the coupling between the ϕ and the neutrinos $g_{\phi\nu} = 3 \times 10^{-8}$, which is consistent with our BP2. The most important aspect in Fig. 5 is the absence of the electron spectra due to the capture of ν_3 which would otherwise appear as a smaller bump just right of the existing ones shown in red and blue bumps. This is due to the fact that the propagation time of the neutrinos between decoupling and detection is much larger than the time after which ν_3 decays. This is direct result of the order of magnitude of $g_{\phi\nu}$ that we consider in our work. Hence, in such a case, CNB consists only of ν_1 and ν_2 . It is to be noted here that we consider normal ordering of neutrino masses here. Furthermore, we assume that ν_2 does not decay to ν_1 in significant amount due to their masses being very close to each other. It is to be noted here that, in the general case, the couplings between the different mass eigenstates of the neutrinos and the scalar could be different. However, in this study, we consider all of them to be same. Although, other decay processes could also take place, we only focus on the decay of the heaviest neutrino eigenstate. The dashed red and blue lines denote the electron spectra due

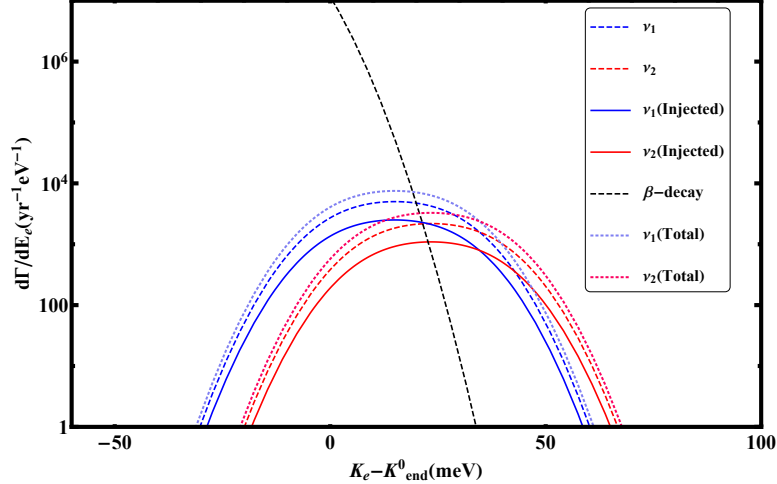


Figure 5: The prediction of differential energy spectra of electron due to the capture of the CNB neutrinos on tritium in PTOLEMY. In this figure dashed, solid and dotted lines correspond to the neutrinos which were present since the decoupling, the neutrinos which are a product of the visible decay and the sum of them respectively. Also here red and blue signifies ν_2 and ν_1 respectively and the black dashed line corresponds to the β decay background. Furthermore, we have considered $\Delta = 40$ meV, $m_{\nu_3} = 50$ meV, $m_\phi = 0.001$ meV, and $g_{\phi\nu} = 3 \times 10^{-8}$.

to the capture of ν_2 and ν_1 respectively which have been a part of the original composition from the time of the decoupling of neutrinos. The solid red and blue lines correspond to the electron spectra due to the capture of ν_2 and ν_1 which were injected to the CNB as a result of the decay of the heavier ν_3 . Finally, the dotted light red and light blue lines correspond to the electron spectra due to the capture of the total ν_2 and ν_1 respectively.

It is to be noted here, that we show the effects on the CNB for only one of our four benchmark cases (BP 2) because in all the other cases as well, the electron spectra would look almost identical. This is due to the fact that as the coupling between neutrino and the scalar $g_{\phi\nu}$ is more than $\mathcal{O}(10^{-15})$, all the ν_3 effectively decay before it reaches the detector. See Ref. [107] for further details on this.

Finally, we would like to mention that the range of the coupling we are operating at in this study, makes PTOLEMY the only experiment in which the effects can be seen in future. This is because the solar neutrino experiments are not sensitive to coupling below $\mathcal{O}(10^{-4})$ and the long baseline experiments are not sensitive to coupling below $\mathcal{O}(0.1)$. Therefore, though there are currently many challenges in front of PTOLEMY, it is still our best hope to probe Yukawa couplings between active neutrinos and ultra-light scalar below $\mathcal{O}(10^{-5})$.

4 Summary and Conclusion

In this article, we have prescribed a method to study the properties of ultra-light scalars, such as mass and the coupling with active neutrinos, through multi-messenger astronomy. The two messengers that we have focussed on are gravitational waves and neutrinos. We have considered a scenario where a rotating BH superradiates and creates a cloud of ultra-light scalars around it. This cloud then creates GW through annihilation of scalars to graviton and neutrinos through a Yukawa coupling with the active neutrinos.

The strain of GW generated in this method is proportional to the mass and the difference between the initial and final spin of the BH and inversely proportional to the luminosity distance of the source. We also observe that the frequency of the GW is inversely proportional to the mass of the BH. Most of the superradiance process is governed by the gravitational fine structure constant which is proportional to the product of the BH mass and the mass of the ultra-light scalar. This constant roughly gives an estimate of the ratio between the dimension of the BH and the compton wavelength of the scalar. It is to be noted here, that there are many other processes through which GW can be created from superradiated bosonic cloud, such as energy level transition of the gravitational atom, bosonova, etc. Here we just focus on the ultra-light scalar annihilation into graviton. Along with all the variables on which the GW depends on, neutrino flux and energy also depend on the coupling with scalar. The neutrino energy increases with the scalar mass, the initial spin of the BH and the gravitational fine structure constant and decreases with the coupling. For the neutrino flux, we identify that it increases with the gravitational fine structure constant and the initial spin of the BH but it decreases with the coupling and the luminosity distance of the source.

We have shown the simultaneous dependence of the properties of the two different messengers on different parameters of the system, e.g. the dependence of the GW frequency and the energy of the neutrinos on the coupling and the strain of the GW and the neutrino flux on the mass of the ultra-light scalar. We take four benchmark cases, where we consider a few values for the coupling, the gravitational fine structure constant, the mass, initial spin, and the luminosity distance of the source. In all our benchmark cases, the gravitational fine structure constant is $\mathcal{O}(0.2)$ and the difference between initial and final BH spin is 0.5. We identify that for different masses of the source BH varying from $10^{-6}M_{\odot}$ to 10^6M_{\odot} there will be GW signals detectable by future GW detectors such as ET, LISA, GB, etc. However, the energy of the neutrinos are always on the higher end, i.e. between TeV to EeV, for the benchmark cases that we have considered. Finally, we show the effect of such coupling between the neutrinos and the ultra-light scalars in the electron spectra due to the capture of CNB neutrinos in PTOLEMY. We find that for couplings $\mathcal{O}(10^{-10})$ or higher, CNB will not consist of ν_3 as all the ν_3 would have essentially decayed to the lighter neutrino eigenstates.

We would like to mention that though we have worked with the superradiated scalar fields, some of the same effects could have also been generated with vector and tensor fields of the appropriate mass and couplings. Also, the possibility of the existence of one or more sterile neutrino species can give rise to a different neutrino flux and energy and also modify the CNB spectra from possible 3-body decays. Finally, with the upcoming high precision GW detectors and neutrino observatories, the burgeoning field of multi-messenger astronomy in near future will be able to test many such possibilities.

Acknowledgments

IKB and SB thank Anna John for useful discussions. IKB acknowledges the support by the MHRD, Government of India, under the Prime Minister's Research Fellows (PMRF) Scheme, 2022.

References

- [1] SAGE collaboration, *Solar neutrino results from SAGE*, *Nucl. Phys. B Proc. Suppl.* **77** (1999) 20.

- [2] MINIBoONE, SciBoONE collaboration, *Dual baseline search for muon antineutrino disappearance at $0.1\text{eV}^2 < \Delta m^2 < 100\text{eV}^2$* , *Phys. Rev. D* **86** (2012) 052009 [[1208.0322](#)].
- [3] SciBoONE, MINIBoONE collaboration, *Dual baseline search for muon neutrino disappearance at $0.5\text{eV}^2 < \Delta m^2 < 40\text{eV}^2$* , *Phys. Rev. D* **85** (2012) 032007 [[1106.5685](#)].
- [4] BOREXINO collaboration, *Final results of Borexino Phase-I on low energy solar neutrino spectroscopy*, *Phys. Rev. D* **89** (2014) 112007 [[1308.0443](#)].
- [5] DUNE collaboration, *Prospects for beyond the Standard Model physics searches at the Deep Underground Neutrino Experiment*, *Eur. Phys. J. C* **81** (2021) 322 [[2008.12769](#)].
- [6] HYPER-KAMIOKANDE collaboration, *Hyper-Kamiokande Design Report*, [1805.04163](#).
- [7] KAMLAND collaboration, *^7Be Solar Neutrino Measurement with KamLAND*, *Phys. Rev. C* **92** (2015) 055808 [[1405.6190](#)].
- [8] SNO collaboration, *Combined Analysis of all Three Phases of Solar Neutrino Data from the Sudbury Neutrino Observatory*, *Phys. Rev. C* **88** (2013) 025501 [[1109.0763](#)].
- [9] MICROBoONE collaboration, *Design and Construction of the MicroBooNE Detector*, *JINST* **12** (2017) P02017 [[1612.05824](#)].
- [10] T2K collaboration, *The T2K Experiment*, *Nucl. Instrum. Meth. A* **659** (2011) 106 [[1106.1238](#)].
- [11] ICECUBE collaboration, *Evidence for High-Energy Extraterrestrial Neutrinos at the IceCube Detector*, *Science* **342** (2013) 1242856 [[1311.5238](#)].
- [12] ICECUBE collaboration, *First observation of PeV-energy neutrinos with IceCube*, *Phys. Rev. Lett.* **111** (2013) 021103 [[1304.5356](#)].
- [13] ICAL collaboration, *Physics Potential of the ICAL detector at the India-based Neutrino Observatory (INO)*, *Pramana* **88** (2017) 79 [[1505.07380](#)].
- [14] RNO-G collaboration, *Searching for cosmic-ray air showers with RNO-G*, *PoS ICRC2023* (2023) 259.
- [15] NOVA collaboration, *The NOvA Technical Design Report*, .
- [16] KAMIOKANDE collaboration, *Atmospheric Neutrino Background and Pion Nuclear Effect for Kamioka Neutron Decay Experiment*, *J. Phys. Soc. Jap.* **55** (1986) 3786.
- [17] K2K collaboration, *Design, construction, and operation of SciFi tracking detector for K2K experiment*, *Nucl. Instrum. Meth. A* **453** (2000) 165 [[hep-ex/0004024](#)].
- [18] ANTARES collaboration, *A deep sea telescope for high-energy neutrinos*, [astro-ph/9907432](#).
- [19] MINOS collaboration, *The MINOS Detectors Technical Design Report*, .
- [20] K. Anderson et al., *The NuMI Facility Technical Design Report*, .
- [21] CHOOZ collaboration, *Initial results from the CHOOZ long baseline reactor neutrino oscillation experiment*, *Phys. Lett. B* **420** (1998) 397 [[hep-ex/9711002](#)].
- [22] SUPER-KAMIOKANDE collaboration, *Measurement of a small atmospheric muon-neutrino / electron-neutrino ratio*, *Phys. Lett. B* **433** (1998) 9 [[hep-ex/9803006](#)].
- [23] ICECUBE-GEN2 collaboration, *IceCube-Gen2: the window to the extreme Universe*, *J. Phys. G* **48** (2021) 060501 [[2008.04323](#)].
- [24] DAYA BAY collaboration, *A Precision measurement of the neutrino mixing angle θ_{13} using reactor antineutrinos at Daya-Bay*, [hep-ex/0701029](#).
- [25] FREJUS collaboration, *Determination of the atmospheric neutrino spectra with the Frejus detector*, *Z. Phys. C* **66** (1995) 417.

- [26] RENO collaboration, *Measurement of Reactor Antineutrino Oscillation Amplitude and Frequency at RENO*, *Phys. Rev. Lett.* **121** (2018) 201801 [[1806.00248](#)].
- [27] E. Andres et al., *The AMANDA neutrino telescope: Principle of operation and first results*, *Astropart. Phys.* **13** (2000) 1 [[astro-ph/9906203](#)].
- [28] I. De Bonis et al., *LBNO-DEMO: Large-scale neutrino detector demonstrators for phased performance assessment in view of a long-baseline oscillation experiment*, [1409.4405](#).
- [29] KM3NET collaboration, *Sensitivity of the KM3NeT/ARCA neutrino telescope to point-like neutrino sources*, *Astropart. Phys.* **111** (2019) 100 [[1810.08499](#)].
- [30] GRAND collaboration, *The Giant Radio Array for Neutrino Detection (GRAND): Science and Design*, *Sci. China Phys. Mech. Astron.* **63** (2020) 219501 [[1810.09994](#)].
- [31] E. Waxman and J.N. Bahcall, *High-energy neutrinos from cosmological gamma-ray burst fireballs*, *Phys. Rev. Lett.* **78** (1997) 2292 [[astro-ph/9701231](#)].
- [32] E. Waxman and J.N. Bahcall, *High-energy neutrinos from astrophysical sources: An Upper bound*, *Phys. Rev. D* **59** (1999) 023002 [[hep-ph/9807282](#)].
- [33] SUPER-KAMIOKANDE collaboration, *Search for supernova relic neutrinos at SUPER-KAMIOKANDE*, *Phys. Rev. Lett.* **90** (2003) 061101 [[hep-ex/0209028](#)].
- [34] D.N. Schramm and G. Steigman, *Relic Neutrinos and the Density of the Universe*, *Astrophys. J.* **243** (1981) 1.
- [35] G. Barr, T.K. Gaisser and T. Stanev, *Flux of Atmospheric Neutrinos*, *Phys. Rev. D* **39** (1989) 3532.
- [36] G. Bellini, A. Ianni, L. Ludhova, F. Mantovani and W.F. McDonough, *Geo-neutrinos*, *Prog. Part. Nucl. Phys.* **73** (2013) 1 [[1310.3732](#)].
- [37] A. Mirizzi, I. Tamborra, H.-T. Janka, N. Saviano, K. Scholberg, R. Bollig et al., *Supernova Neutrinos: Production, Oscillations and Detection*, *Riv. Nuovo Cim.* **39** (2016) 1 [[1508.00785](#)].
- [38] R. Davis, Jr., D.S. Harmer and K.C. Hoffman, *Search for neutrinos from the sun*, *Phys. Rev. Lett.* **20** (1968) 1205.
- [39] SUPER-KAMIOKANDE collaboration, *Solar Neutrino Measurements in Super-Kamiokande-IV*, *Phys. Rev. D* **94** (2016) 052010 [[1606.07538](#)].
- [40] SNO collaboration, *Direct evidence for neutrino flavor transformation from neutral current interactions in the Sudbury Neutrino Observatory*, *Phys. Rev. Lett.* **89** (2002) 011301 [[nucl-ex/0204008](#)].
- [41] K. Griest and M. Kamionkowski, *Unitarity Limits on the Mass and Radius of Dark Matter Particles*, *Phys. Rev. Lett.* **64** (1990) 615.
- [42] E.G.M. Ferreira, *Ultra-light dark matter*, *Astron. Astrophys. Rev.* **29** (2021) 7 [[2005.03254](#)].
- [43] A. Arvanitaki, S. Dimopoulos, S. Dubovsky, N. Kaloper and J. March-Russell, *String Axiverse*, *Phys. Rev. D* **81** (2010) 123530 [[0905.4720](#)].
- [44] P.J.E. Peebles and B. Ratra, *The Cosmological Constant and Dark Energy*, *Rev. Mod. Phys.* **75** (2003) 559 [[astro-ph/0207347](#)].
- [45] E. Fischbach, G.T. Gillies, D.E. Krause, J.G. Schwan and C. Talmadge, *Nonnewtonian gravity and new weak forces: An Index of measurements and theory*, *Metrologia* **29** (1992) 213.
- [46] S.M. Carroll, G.B. Field and R. Jackiw, *Limits on a Lorentz and Parity Violating Modification of Electrodynamics*, *Phys. Rev. D* **41** (1990) 1231.
- [47] S.M. Carroll and G.B. Field, *The Einstein equivalence principle and the polarization of radio galaxies*, *Phys. Rev. D* **43** (1991) 3789.

- [48] D. Harari and P. Sikivie, *Effects of a Nambu-Goldstone boson on the polarization of radio galaxies and the cosmic microwave background*, *Phys. Lett. B* **289** (1992) 67.
- [49] G. Raffelt and L. Stodolsky, *Mixing of the Photon with Low Mass Particles*, *Phys. Rev. D* **37** (1988) 1237.
- [50] A. Arvanitaki and S. Dubovsky, *Exploring the String Axiverse with Precision Black Hole Physics*, *Phys. Rev. D* **83** (2011) 044026 [[1004.3558](#)].
- [51] Y. Chen, X. Xue and V. Cardoso, *Black Holes as Neutrino Factories*, [2308.00741](#).
- [52] G.B. Gelmini and M. Roncadelli, *Left-Handed Neutrino Mass Scale and Spontaneously Broken Lepton Number*, *Phys. Lett. B* **99** (1981) 411.
- [53] H. Georgi and S.L. Glashow, *Unity of All Elementary Particle Forces*, *Phys. Rev. Lett.* **32** (1974) 438.
- [54] J.C. Pati and A. Salam, *Lepton Number as the Fourth Color*, *Phys. Rev. D* **10** (1974) 275.
- [55] R.N. Mohapatra and J.C. Pati, *Left-Right Gauge Symmetry and an Isoconjugate Model of CP Violation*, *Phys. Rev. D* **11** (1975) 566.
- [56] J.D. Bekenstein, *Extraction of energy and charge from a black hole*, *Phys. Rev. D* **7** (1973) 949.
- [57] J.D. Bekenstein and M. Schiffer, *The Many faces of superradiance*, *Phys. Rev. D* **58** (1998) 064014 [[gr-qc/9803033](#)].
- [58] S.L. Detweiler, *KLEIN-GORDON EQUATION AND ROTATING BLACK HOLES*, *Phys. Rev. D* **22** (1980) 2323.
- [59] LIGO SCIENTIFIC, VIRGO collaboration, *Observation of Gravitational Waves from a Binary Black Hole Merger*, *Phys. Rev. Lett.* **116** (2016) 061102 [[1602.03837](#)].
- [60] NANOGrav collaboration, *The NANOGrav 15 yr Data Set: Evidence for a Gravitational-wave Background*, *Astrophys. J. Lett.* **951** (2023) L8 [[2306.16213](#)].
- [61] NANOGrav collaboration, *The NANOGrav 15 yr Data Set: Observations and Timing of 68 Millisecond Pulsars*, *Astrophys. J. Lett.* **951** (2023) L9 [[2306.16217](#)].
- [62] EPTA, INPTA: collaboration, *The second data release from the European Pulsar Timing Array - III. Search for gravitational wave signals*, *Astron. Astrophys.* **678** (2023) A50 [[2306.16214](#)].
- [63] EPTA collaboration, *The second data release from the European Pulsar Timing Array - I. The dataset and timing analysis*, *Astron. Astrophys.* **678** (2023) A48 [[2306.16224](#)].
- [64] EPTA collaboration, *The second data release from the European Pulsar Timing Array: V. Implications for massive black holes, dark matter and the early Universe*, [2306.16227](#).
- [65] D.J. Reardon et al., *Search for an Isotropic Gravitational-wave Background with the Parkes Pulsar Timing Array*, *Astrophys. J. Lett.* **951** (2023) L6 [[2306.16215](#)].
- [66] A. Zic et al., *The Parkes Pulsar Timing Array third data release*, *Publ. Astron. Soc. Austral.* **40** (2023) e049 [[2306.16230](#)].
- [67] D.J. Reardon et al., *The Gravitational-wave Background Null Hypothesis: Characterizing Noise in Millisecond Pulsar Arrival Times with the Parkes Pulsar Timing Array*, *Astrophys. J. Lett.* **951** (2023) L7 [[2306.16229](#)].
- [68] H. Xu et al., *Searching for the Nano-Hertz Stochastic Gravitational Wave Background with the Chinese Pulsar Timing Array Data Release I*, *Res. Astron. Astrophys.* **23** (2023) 075024 [[2306.16216](#)].
- [69] LISA collaboration, *Laser Interferometer Space Antenna*, [1702.00786](#).

- [70] W.-H. Ruan, Z.-K. Guo, R.-G. Cai and Y.-Z. Zhang, *Taiji program: Gravitational-wave sources*, *Int. J. Mod. Phys. A* **35** (2020) 2050075 [[1807.09495](#)].
- [71] S. Kawamura et al., *The Japanese space gravitational wave antenna: DECIGO*, *Class. Quant. Grav.* **28** (2011) 094011.
- [72] S.P. et al., *The Big Bang Observer: Direct detection of gravitational waves from the birth of the Universe to the Present*, *NASA Mission Concept Study* (2004) .
- [73] M. Punturo et al., *The Einstein Telescope: A third-generation gravitational wave observatory*, *Class. Quant. Grav.* **27** (2010) 194002.
- [74] D. Reitze et al., *Cosmic Explorer: The U.S. Contribution to Gravitational-Wave Astronomy beyond LIGO*, *Bull. Am. Astron. Soc.* **51** (2019) 035 [[1907.04833](#)].
- [75] A. Arvanitaki and A.A. Geraci, *Detecting high-frequency gravitational waves with optically-levitated sensors*, *Phys. Rev. Lett.* **110** (2013) 071105 [[1207.5320](#)].
- [76] N. Aggarwal, G.P. Winstone, M. Teo, M. Baryakhtar, S.L. Larson, V. Kalogera et al., *Searching for New Physics with a Levitated-Sensor-Based Gravitational-Wave Detector*, *Phys. Rev. Lett.* **128** (2022) 111101 [[2010.13157](#)].
- [77] M.E. Gertsenshtein, *Wave resonance of light and gravitational waves*, *Soviet Physics JETP* **14** (1962) 84.
- [78] J.R. et al., *Next Generation Search for Axion and ALP Dark Matter with the International Axion Observatory*, *2018 IEEE Nuclear Science Symposium and Medical Imaging Conference* (2018) 8824640.
- [79] R. Bähre et al., *Any light particle search II — Technical Design Report*, *JINST* **8** (2013) T09001 [[1302.5647](#)].
- [80] C. Albrecht, S. Barbanotti, H. Hintz, K. Jensch, R. Klos, W. Maschmann et al., *Straightening of Superconducting HERA Dipoles for the Any-Light-Particle-Search Experiment ALPS II*, *EPJ Tech. Instrum.* **8** (2021) 5 [[2004.13441](#)].
- [81] S. Chaudhuri, P.W. Graham, K. Irwin, J. Mardon, S. Rajendran and Y. Zhao, *Radio for hidden-photon dark matter detection*, *Phys. Rev. D* **92** (2015) 075012 [[1411.7382](#)].
- [82] M. Silva-Feaver et al., *Design Overview of DM Radio Pathfinder Experiment*, *IEEE Trans. Appl. Supercond.* **27** (2017) 1400204 [[1610.09344](#)].
- [83] HOLOMETER collaboration, *MHz Gravitational Wave Constraints with Decameter Michelson Interferometers*, *Phys. Rev. D* **95** (2017) 063002 [[1611.05560](#)].
- [84] T. Akutsu et al., *Search for a stochastic background of 100-MHz gravitational waves with laser interferometers*, *Phys. Rev. Lett.* **101** (2008) 101101 [[0803.4094](#)].
- [85] F.-Y. Li, M.-X. Tang and D.-P. Shi, *Electromagnetic response of a Gaussian beam to high frequency relic gravitational waves in quintessential inflationary models*, *Phys. Rev. D* **67** (2003) 104008 [[gr-qc/0306092](#)].
- [86] F.-Y. Li and N. Yang, *Resonant interaction between a weak gravitational wave and a microwave beam in the double polarized states through a static magnetic field*, *Chin. Phys. Lett.* **21** (2004) 2113 [[gr-qc/0410060](#)].
- [87] F. Li, R.M.L. Baker, Jr. and Z. Chen, *Perturbative photon flux generated by high-frequency relic gravitational waves and utilization of them for their detection*, [gr-qc/0604109](#).
- [88] D.J. Fixsen et al., *ARCADE 2 Measurement of the Extra-Galactic Sky Temperature at 3-90 GHz*, *Astrophys. J.* **734** (2011) 5 [[0901.0555](#)].
- [89] J.D. Bowman, A.E.E. Rogers, R.A. Monsalve, T.J. Mozdzen and N. Mahesh, *An absorption profile centred at 78 megahertz in the sky-averaged spectrum*, *Nature* **555** (2018) 67 [[1810.05912](#)].

- [90] R. Brito, V. Cardoso and P. Pani, *Superradiance: New Frontiers in Black Hole Physics*, *Lect. Notes Phys.* **906** (2015) pp.1 [[1501.06570](#)].
- [91] H. Yoshino and H. Kodama, *Bosenova collapse of axion cloud around a rotating black hole*, *Prog. Theor. Phys.* **128** (2012) 153 [[1203.5070](#)].
- [92] H. Yoshino and H. Kodama, *Gravitational radiation from an axion cloud around a black hole: Superradiant phase*, *PTEP* **2014** (2014) 043E02 [[1312.2326](#)].
- [93] J.M. Berryman et al., *Neutrino self-interactions: A white paper*, *Phys. Dark Univ.* **42** (2023) 101267 [[2203.01955](#)].
- [94] M. Kachelriess, R. Tomas and J.W.F. Valle, *Supernova bounds on Majoron emitting decays of light neutrinos*, *Phys. Rev. D* **62** (2000) 023004 [[hep-ph/0001039](#)].
- [95] Y. Farzan, *Bounds on the coupling of the Majoron to light neutrinos from supernova cooling*, *Phys. Rev. D* **67** (2003) 073015 [[hep-ph/0211375](#)].
- [96] F. Forastieri, M. Lattanzi and P. Natoli, *Constraints on secret neutrino interactions after Planck*, *JCAP* **07** (2015) 014 [[1504.04999](#)].
- [97] F. Forastieri, M. Lattanzi and P. Natoli, *Cosmological constraints on neutrino self-interactions with a light mediator*, *Phys. Rev. D* **100** (2019) 103526 [[1904.07810](#)].
- [98] J. Venzor, G. Garcia-Arroyo, A. Pérez-Lorenzana and J. De-Santiago, *Massive neutrino self-interactions with a light mediator in cosmology*, *Phys. Rev. D* **105** (2022) 123539 [[2202.09310](#)].
- [99] K. El-Badry et al., *A Sun-like star orbiting a black hole*, *Mon. Not. Roy. Astron. Soc.* **518** (2023) 1057 [[2209.06833](#)].
- [100] ICECUBE collaboration, *Evidence for neutrino emission from the nearby active galaxy NGC 1068*, *Science* **378** (2022) 538 [[2211.09972](#)].
- [101] ICECUBE collaboration, *Observation of high-energy neutrinos from the Galactic plane*, *Science* **380** (2023) adc9818 [[2307.04427](#)].
- [102] ICECUBE collaboration, *An absence of neutrinos associated with cosmic-ray acceleration in γ -ray bursts*, *Nature* **484** (2012) 351 [[1204.4219](#)].
- [103] R. Stein et al., *A tidal disruption event coincident with a high-energy neutrino*, *Nature Astron.* **5** (2021) 510 [[2005.05340](#)].
- [104] S. van Velzen et al., *Establishing accretion flares from massive black holes as a major source of high-energy neutrinos*, [2111.09391](#).
- [105] A. Acker, S. Pakvasa and J.T. Pantaleone, *Decaying Dirac neutrinos*, *Phys. Rev. D* **45** (1992) 1.
- [106] A. Acker and S. Pakvasa, *Solar neutrino decay*, *Phys. Lett. B* **320** (1994) 320 [[hep-ph/9310207](#)].
- [107] K. Akita, G. Lambiase and M. Yamaguchi, *Unstable cosmic neutrino capture*, *JHEP* **02** (2022) 132 [[2109.02900](#)].
- [108] PTOLEMY collaboration, *PTOLEMY: A Proposal for Thermal Relic Detection of Massive Neutrinos and Directional Detection of MeV Dark Matter*, [1808.01892](#).
- [109] Y. Cheipesh, V. Cheianov and A. Boyarsky, *Navigating the pitfalls of relic neutrino detection*, *Phys. Rev. D* **104** (2021) 116004 [[2101.10069](#)].
- [110] PTOLEMY collaboration, *Heisenberg's uncertainty principle in the PTOLEMY project: A theory update*, *Phys. Rev. D* **106** (2022) 053002 [[2203.11228](#)].